Supporting information for "Quantifying the impact of the Three Gorges Dam on the thermal dynamics in the Yangtze River"

Huayang Cai[1], Sebastiano Piccolroaz[2,3], Jingzheng Huang[1], Zhiyong Liu[4], Feng Liu[1,5], and Marco Toffolon[3]

[1] Institute of Estuarine and Coastal Research, School of Marine Sciences, Sun Yat-sen University, Guangzhou 510275, China

[2] Institute for Marine and Atmospheric research, Department of Physics and Astronomy, Utrecht University, Princetonplein 5, 3584 CC, Utrecht, The Netherlands

[3] Department of Civil, Environmental and Mechanical Engineering, University of Trento, via Mesiano 77 Trento, 38123, Italy

[4] Department/Center of Water Resources and Environment, Sun Yat-sen University, Guangzhou 510275, China

[5] Author to whom any correspondence should be addressed

E-mail: `liuf53@mail.sysu.edu.cn`

December 2017

Submitted to: *Environ. Res. Lett.*

Text S1. Description of the models

S1.1 Hybrid model for river water temperature (air2stream)

The *air2stream* model (Toffolon & Piccolroaz, 2015, the source code is available at https://github.com/marcotoffolon/air2stream) is a hybrid model that allows for forecasting the river water temperature (RWT, indicated by the variable T_w) as a function of air temperature (AT, indicated by T_a) and river discharge (Q) on daily time scale. The model considers an unspecified volume V of the river reach, the potential influence of upstream tributaries (and possibly groundwater), and the energy exchange with the atmosphere. The lumped energy budget equation is described as follows:

$$\rho c_p V \frac{\mathrm{d}T_w}{\mathrm{d}t} = A\,H + \rho c_p \left(\sum_i Q_i T_{w,i} - Q T_w \right) , \tag{S1}$$

where t is time, ρ is water density, c_p is specific heat at constant pressure, A is the surface area of the river reach, and Q_i and $T_{w,i}$ are freshwater discharge and temperature of the i-th contributing water flux generated by tributaries or groundwater. The net energy flux at the river-atmosphere interface is lumped into the parameter H, which implicitly accounts for the contributions of the main heat flux components, including short-wave and long-wave radiation, latent and sensible heat fluxes. Introducing some broad simplifications (for details see Toffolon & Piccolroaz, 2015), the daily thermal dynamics can be described by the final form of the model in its full version (with 8 parameters, a_1-a_8)

$$\begin{aligned} \frac{\mathrm{d}T_w}{\mathrm{d}t} &= \frac{1}{\delta} \left\{ a_1 + a_2 T_a - a_3 T_w + \theta \left[a_5 + a_6 \cos(2\pi(t/t_y - a_7)) - a_8 T_w \right] \right\} \\ \delta = \theta^{a_4}, &\quad \theta = Q/\overline{Q}. \end{aligned} \tag{S2}$$

where t_y is the duration of one year in the units used for time, and θ is the dimensionless river discharge, with $\overline{Q} = (t_2 - t_1)^{-1} \int_{t_1}^{t_2} Q(t)\mathrm{d}t$ being a reference value averaged over the long-term time series (between t_1 and t_2). The parameter δ is the dimensionless reference depth following a simple power law as a function of the discharge.

The ordinary differential equation (S2) is solved numerically using the second-order accurate Crank-Nicolson scheme with a time step of one day. The lower-bounded value of river water temperature is set to be 0°C. The eight parameters (a_1-a_8), constrained within a physically reasonable range, are estimated by calibration process using a Monte Carlo-based optimization procedure. The objective function adopted for identifying the best set of parameters is the root mean square error (RMSE) between simulated T_w and observed ($\widehat{T_w}$):

$$RMSE = \sqrt{\frac{1}{n} \sum_{j=1}^{n} \left(T_{w,j} - \widehat{T_{w,j}} \right)^2} , \tag{S3}$$

where n is the number of total number of measurements. Generally, the observation series should be long enough in order to capture the inter-annual variability and the possible extreme events (e.g., droughts and floods).

S1.2 Purely statistical model

To illustrate the advantage of the *air2stream* model, we also tested one of the most common nonlinear regression model based on the logistic function (e.g., Mohseni et al., 1998; Arismendi et al., 2014)

$$T_w = \alpha_1 + \frac{\alpha_2 - \alpha_1}{1 + e^{\alpha_3\left(\alpha_4 - \widehat{T_a}\right)}}\,, \tag{S4}$$

which predicts RWT using air temperature alone relying on 4 calibration parameters (i.e., α_1 and α_2 represent the minimum and maximum RWT of the analyzed period of data, respectively, α_3 indicates a measure of the steepest slope of the logistic function, and α_4 represents the air temperature at the inflection point). We estimated T_w at day i using the daily averaged air temperatures $\widehat{T_a}$ at day i and $i-1$ (Toffolon & Piccolroaz, 2015). The values of RMSE of the regression model (S4) are presented in Table S2, which shows that *air2stream* model has a better performance than the logistic regression model (see also Piccolroaz et al. (2016)). For illustration, the calibration results of applying the logistic model (S4) and the *air2stream* model to Cuntan station are displayed in Figure S2 through a scatter plot between simulated and observed RWT. The narrower range of predicted RWT using *air2stream* model indicates a significantly better reproduction of the river's thermal dynamics.

Text S2. Effect of urban wastewater on RWT

In order to illustrate whether the effect of sewage system may be relevant, we used a simple energy balance in equilibrium conditions:

$$\rho c_p Q_u T_u + \rho c_p Q_s T_s = \rho c_p Q_d T_d\,, \tag{S5}$$

where subscript u indicates 'upstream', d indicates 'downstream' and s indicates 'sewage'. Considering also the mass (volume) balance

$$Q_u + Q_s = Q_d\,, \tag{S6}$$

we can compute the downstream RWT

$$T_d = \frac{Q_u T_u + Q_s T_s}{Q_d}\,, \tag{S7}$$

and its alteration relative to upstream conditions

$$T_d - T_u = \frac{Q_s}{Q_d}\left(T_s - T_u\right)\,. \tag{S8}$$

It was shown by Wang et al. (2017) that the averaged discharge ratio (Q_s/Q_d) over the Yangtze River Basin ranged between 1.1% and 2.5% during the period of 1998-2014. Thus, the alteration of RWT along the Yangtze River due to sewage discharge is about 1.1%∼2.5% of the temperature difference between the sewage temperature and the upstream RWT. Chinese regulations dictate that the maximum difference $T_s - T_u$ cannot exceed 8°C, hence the alteration of RWT ($T_d - T_u$) would be around 0.09∼0.2°C.

However, according to the "Chinese Environmental quality standards for surface water" (http://www.mep.gov.cn/gkml/hbb/bgth/200910/W020090724340379457140.pdf, in Chinese), the maximum increase of weekly averaged RWT is 1°C, so the expected impact is on the order of 0.01°C.

Text S3. Length scale of thermal adaptation

Following a water particle transported by the flow, i.e. adopting a Lagrangian description, equation (S1) can be cast in the form

$$\frac{\mathrm{D}T_w}{\mathrm{D}t} = \frac{1}{\rho c_p Y}\,H\,, \tag{S9}$$

where $\mathrm{D}/\mathrm{D}t$ indicates the material (Lagrangian) derivative and $Y = V/A$ the average flow depth. If we assume a disturbance in a given river station (e.g., the TGD), the integration of equation (S9) provides the temporal decay of the disturbance with the propagation of the water downstream. Hence, a temporal time scale of the process, t_{decay}, can be defined and converted into a characteristic length scale, L_{decay}. By assuming, as a first order approximation, steady-state hydrodynamics with a constant and uniform velocity u_0 along the river, the length scale can be easily estimated as

$$L_{decay} = u_0\,t_{decay}\,. \tag{S10}$$

Now, the issue is how to estimate t_{decay} from equation (S9). This would require the computation of all the heat flux terms that contribute to the net flux H, a rather difficult task (Toffolon & Piccolroaz, 2015). However, the calibration of the *air2stream* model already provided meaningful indications about the order of magnitude of the exchange terms with the atmosphere. In this regard, assuming that the external conditions remain constant in the observed period and being aware of the strong simplifications introduced, equation (S2) can be rewritten as

$$\frac{\mathrm{d}T_w}{\mathrm{d}t} = -k\,T_w + \sigma\,, \qquad k = \frac{(a_3 + \theta\,a_8)}{\delta}\,, \tag{S11}$$

where σ summarizes all the external factors, and only the dependence on T_w is explicitly retained, with θ and δ accounting for the effect of the discharge. Equation (S11) allows for a simple analytical solution

$$T_w = \frac{\sigma}{k} + \left(T_{w0} - \frac{\sigma}{k}\right)\exp\left(-k\,t\right)\,, \tag{S12}$$

where the first term at the right hand side represents the equilibrium temperature and the second one the temporal decay of the initial value of RWT, T_{w0}. It is clear that k^{-1} is the time scale of the decay, hence

$$t_{decay} = \frac{\delta}{(a_3 + \theta\,a_8)}\,. \tag{S13}$$

A similar analysis was proposed by Toffolon et al. (2014) for case of lakes using the *air2water* model.

Table S3 reports the calibrated values of the model's parameters together with the estimates of t_{decay} and L_{decay}. In this exercise, we assumed $\theta = \delta = 1$ (corresponding to the the average discharge) and $u_0 \simeq 1.4$ m/s, a reference value estimated from the measurements reported in Lai et al. (2017) for the Yangtze from Yichang to Hankou (about 600 km). The values of t_{decay} and L_{decay} for the three stations downstream of the TGD are on the order of 8 days and 1000 km, respectively. The variations among the stations is relatively small, strengthening the confidence in a local analysis of the model's parameters, instead of solving the Lagrangian model (S9). Incidentally, we note that the long time and length scales are mostly due to the rather large reference depth of the Yangtze ($Y \simeq 14$ m) (Lai et al., 2017), which strongly affects the values of the *air2stream* parameters.

References

Arismendi I Safeeq M Dunham JB Johnson SL (2014). Can air temperature be used to project influences of climate change on stream temperature. Environ. Res. Lett. 9.

Lai X Yin D Finlayson B Wei T Li M Yuan W Yang S Dai Z Gao S Chen Z (2017). Will river erosion below the Three Gorges Dam stop in the middle Yangtze? J. Hydrol. 554:24–31.

Mohseni O Stefan HG R. ET (1998). A nonlinear regression model for weekly stream temperatures. Water Resour. Res. 34:2685–2692.

Piccolroaz S Calamita E Majone B Gallice A Siviglia A Toffolon M (2016). Prediction of river water temperature: a comparison between a new family of hybrid models and statistical approaches. Hydrol. Process. 30:3901–3917.

Toffolon M Piccolroaz S (2015). A hybrid model for river water temperature as a function of air temperature and discharge. Environ. Res. Lett. 10.

Toffolon M Piccolroaz S Majone B Soja AM Peeters F Schmid M Wuest A (2014). Prediction of surface temperature in lakes with different morphology using air temperature. Limnol. Oceanogr. 59:2185–2202.

Wang Z Shao D Westerhoff P (2017). Wastewater discharge impact on drinking water sources along the Yangtze River (China). Sci.Total Environ. 599:1399–1407.

Table S1. Details of the observed data along the Yangtze River.

Stations	Type	Latitude	Longitude	Elevation (m)	Variable	Time series	Distance from the TGD (km)
Cuntan	Hydrological	29.62N	106.60E	-	RWT, Q	1975-1986, 2003-2014	-680 (upstream)
Yichang	Hydrological	30.70N	111.28E	-	RWT, Q	1975-1987, 2003-2014	44 (downstream)
Hankou	Hydrological	30.58N	114.28E	-	RWT, Q	1975-1985, 1987, 2003-2014	645 (downstream)
Datong	Hydrological	29.58N	117.62E	-	RWT, Q	1975-1985, 1987, 2003-2014	1,115 (downstream)
Shapingba	Meteorological	29.58N	106.47E	259	AT	1975-1986, 2003-2014	-
Yichang	Meteorological	30.70N	111.28E	133	AT	1975-1987, 2003-2014	-
Wuhan	Meteorological	30.62N	114.13E	23	AT	1975-1985, 1987, 2003-2014	-
Anqing	Meteorological	30.53N	117.05E	20	AT	1975-1985, 1987, 2003-2014	-

Table S2. Performance of the *air2stream* model (8-parameter version, a2s-8) applied to the four hydrological stations in the Yangtze River, for the pre-GZB (calibration) and post-GZB periods.

Version	RMSE for RWT (°C)							
	Cuntan		Yichang		Hankou		Datong	
	Pre-GZB	Post-GZB	Pre-GZB	Post-GZB	Pre-GZB	Post-GZB	Pre-GZB	Post-GZB
a2s-8	0.57	0.61	0.74	0.75	0.76	1.05	0.69	0.70

Table S3. Parameters of the model resulting from calibration, and values of the temporal and spatial scales t_{decay} and L_{decay}.

	Cuntan	Yichang	Hankou	Datong
a_1 [°C/day]	0.141557	0.218895	0.272358	0.159331
a_2 [day^{-1}]	0.069907	0.043229	0.102467	0.090474
a_3 [day^{-1}]	0.067363	0.042963	0.103939	0.093688
a_4 [-]	0.363315	0.207035	1.08E-07	1.13E-07
a_5 [°C/day]	1.201328	0.912877	0.654284	0.394751
a_6 [°C/day]	0.457173	0.481453	0.332901	0.130254
a_7 [-]	0.543649	0.564069	0.561695	0.523553
a_8 [day^{-1}]	0.075177	0.061340	0.041551	0.020706
t_{decay} [day]	7.0	9.6	6.9	8.7
L_{decay} [km]	849	1160	831	1057

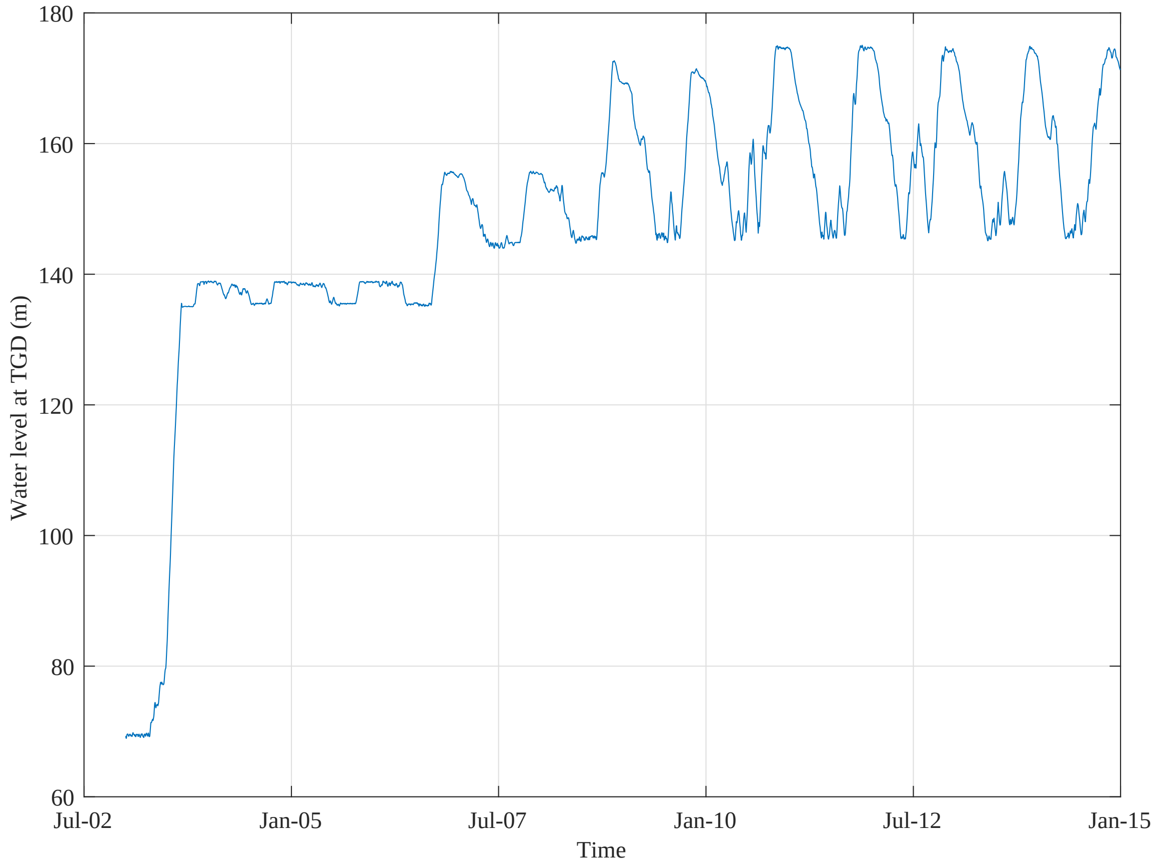

Figure S1. Variations of the operational stage at TGD in the period 2003-2014 (data from official report provided by China Three Gorges Corporation, available at http://www.ctg.com.cn/eportal/fileDir/sxjt/resource/cms/2016/04/20160414170418204 98.pdf).

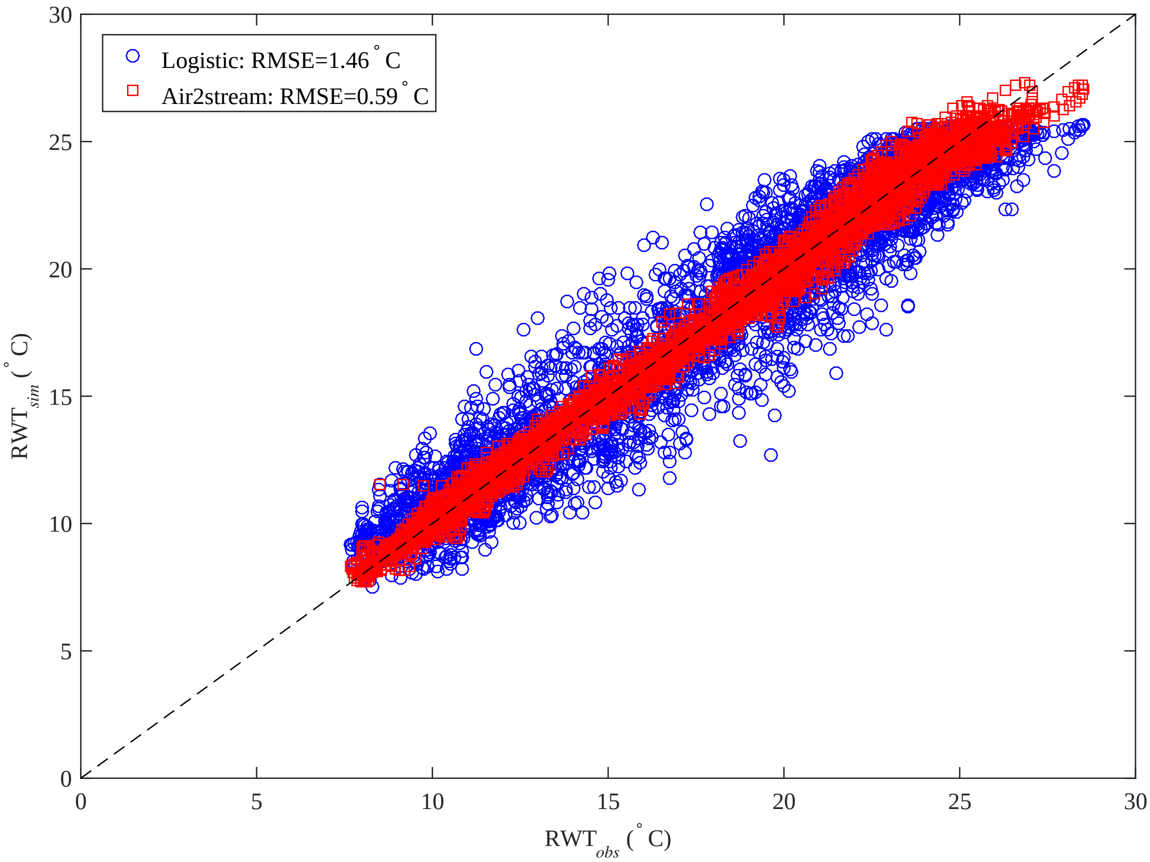

Figure S2. Scatter plot of observed and simulated RWT using the logistic regression and the *air2stream* model for the calibration period of 1975-1986 at Cuntan station.

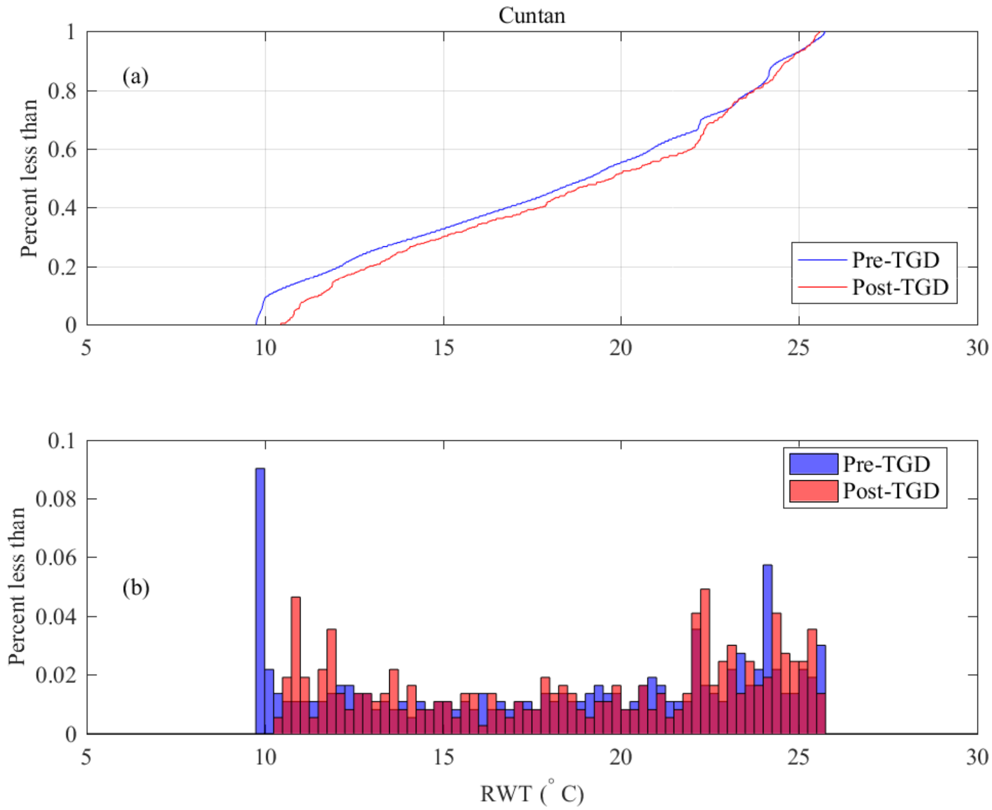

Figure S3. RWT duration curves and histograms constructed at Cuntan station for the pre-TGD and post-TGD periods.

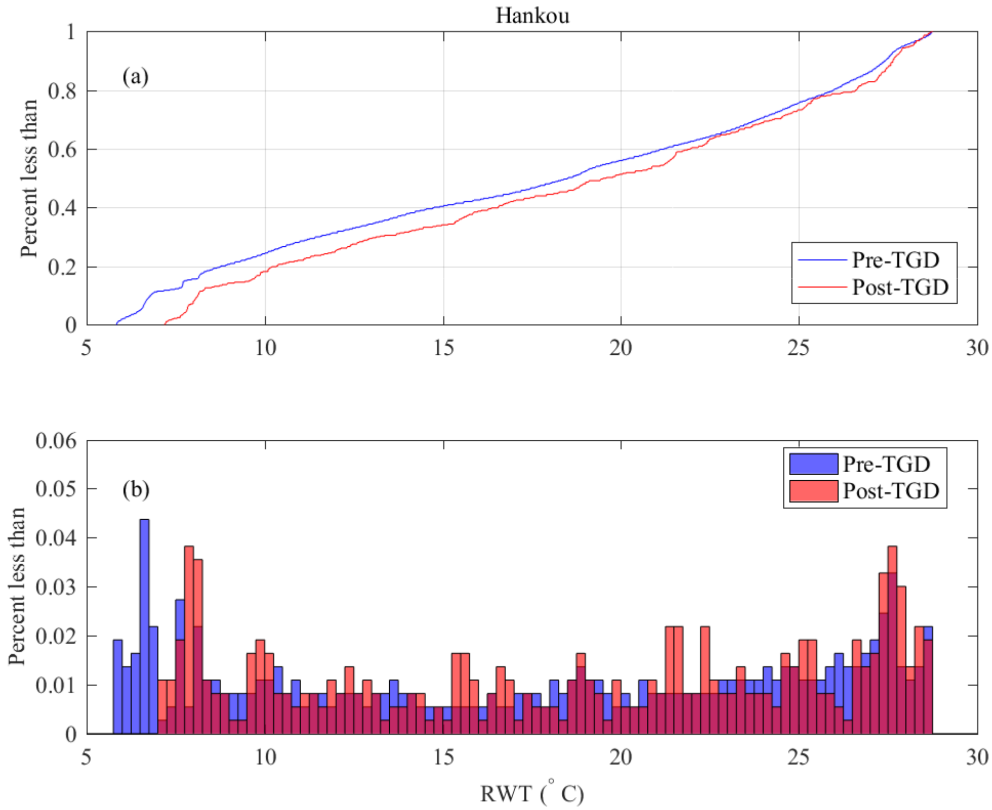

Figure S4. RWT duration curves and histograms constructed at Hankou station for the pre-TGD and post-TGD periods.

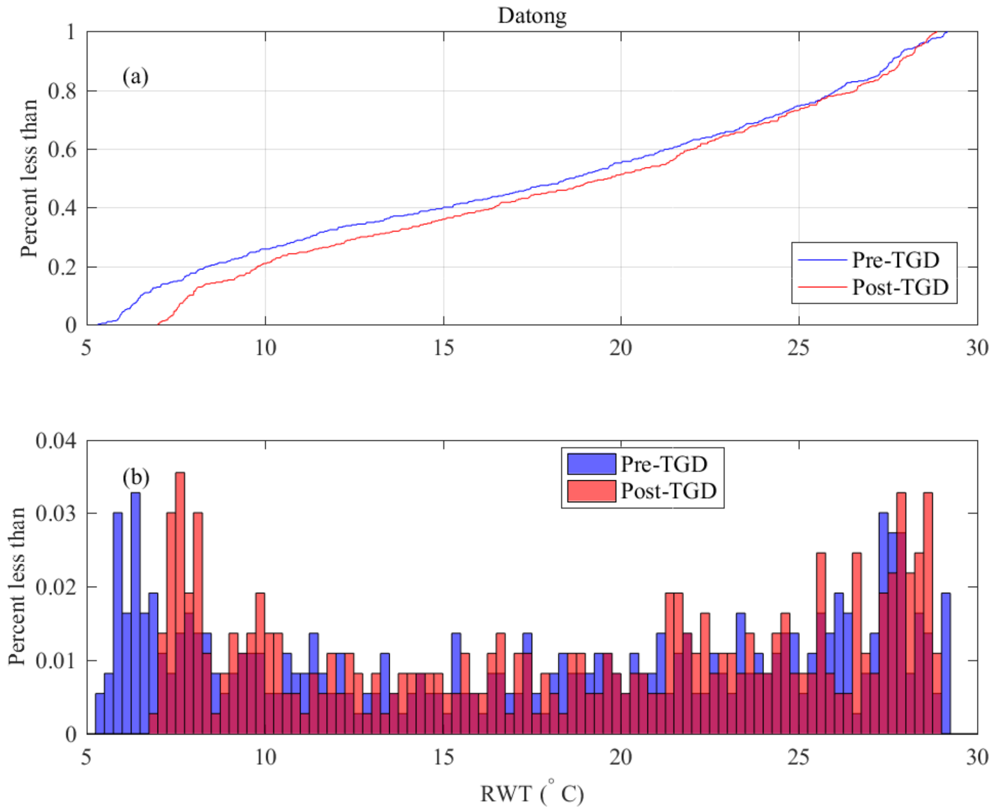

Figure S5. RWT duration curves and histograms constructed at Datong station for the pre-TGD and post-TGD periods.

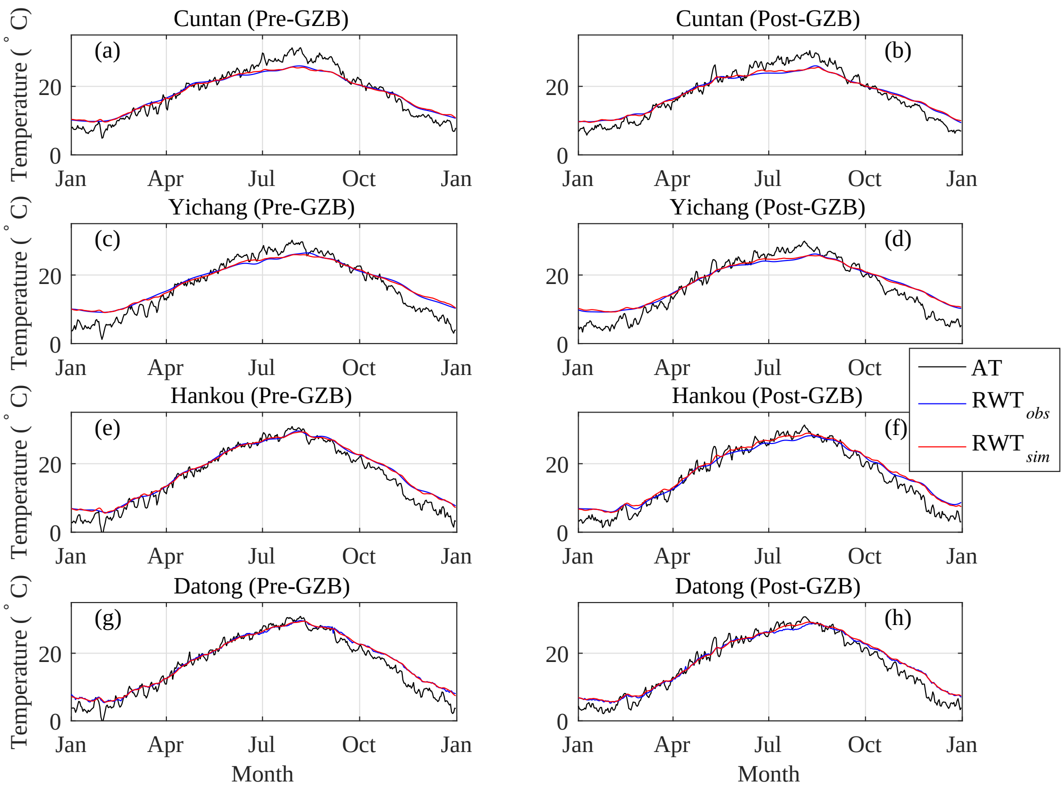

Figure S6. Comparison between observed air temperature (AT), observed RWT (RWT_{obs}), and simulated RWT (RWT_{sim}) at the four hydrological stations for the climatological year, and for (a, c, e, g) the pre-GZB period (used for model calibration) and (b, d, f, h) the post-GZB period (where the model is used in prediction).

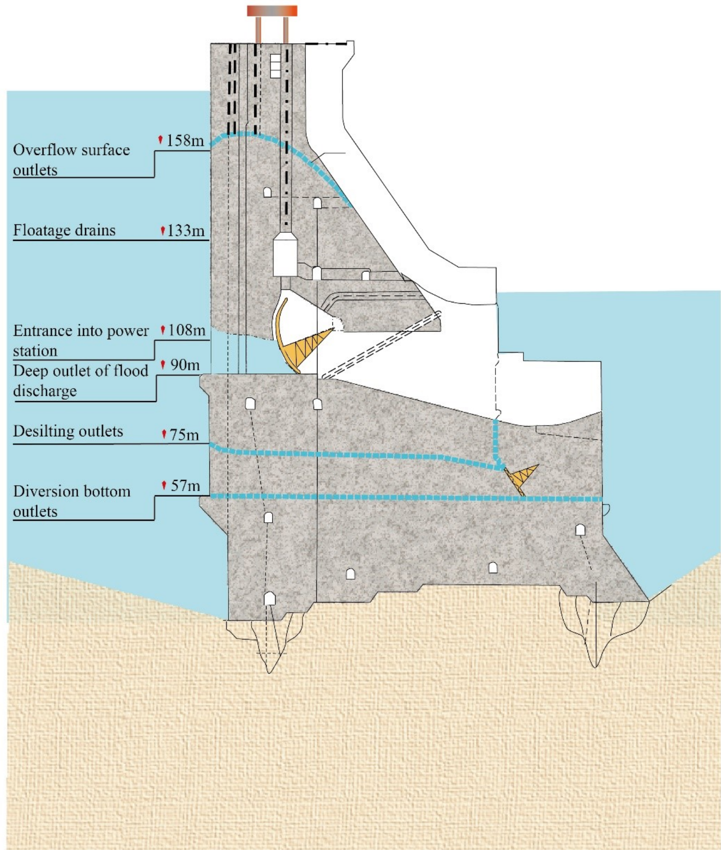

Figure S7. Detail of the distribution of outlets in the TGD and their corresponding elevation relative to the river bed at the dam site (data from http://www.chinawater.com.cn/).

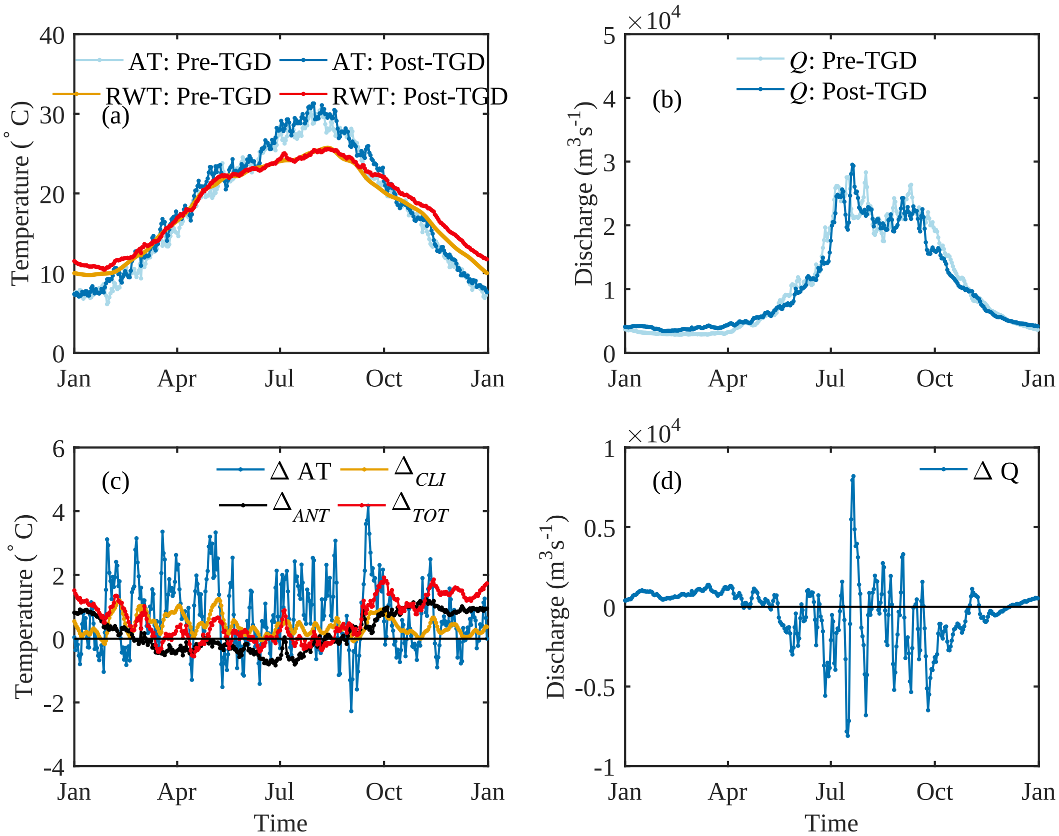

Figure S8. Seasonal dynamics (climatological year) of (a) AT and RWT, and (b) discharge Q, at Cuntan station during pre-TGD and post-TGD periods. Plots (c) and (d) show the differences between the two periods, highlighting the RWT changes caused by meteorological forcing and TGD.

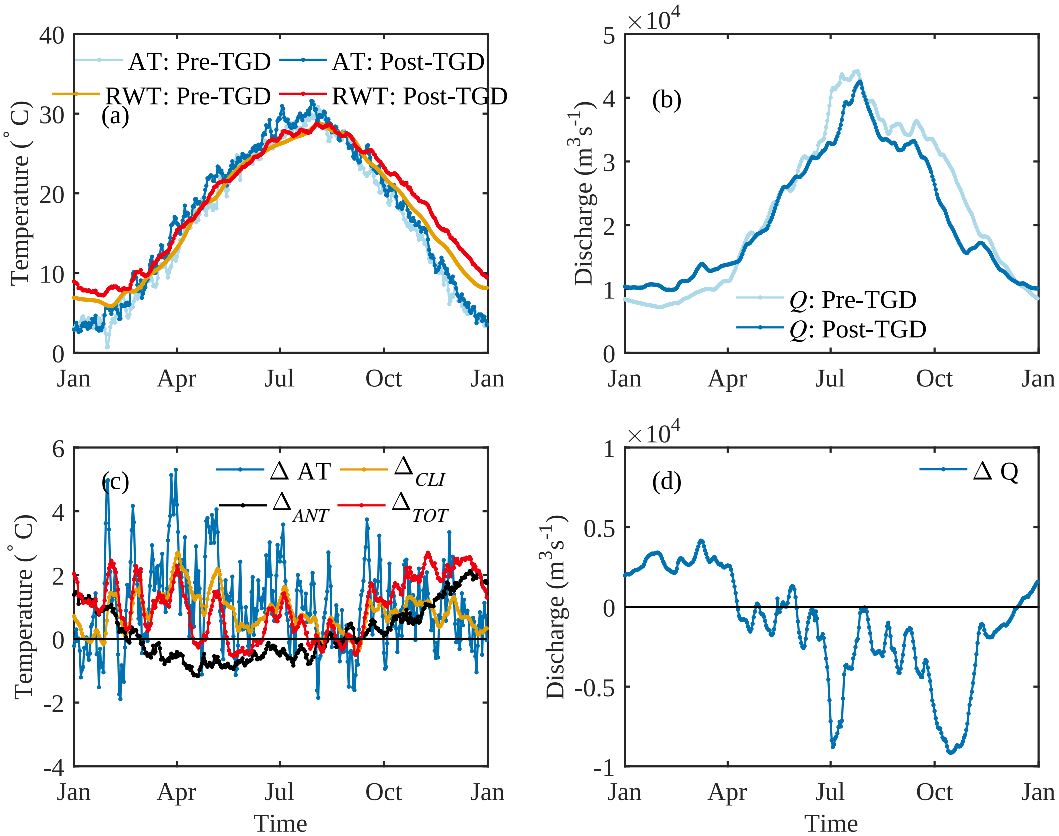

Figure S9. Seasonal dynamics (climatological year) of (a) AT and RWT, and (b) discharge Q, at Hankou station during pre-TGD and post-TGD periods. Plots (c) and (d) show the differences between the two periods, highlighting the RWT changes caused by meteorological forcing and TGD.

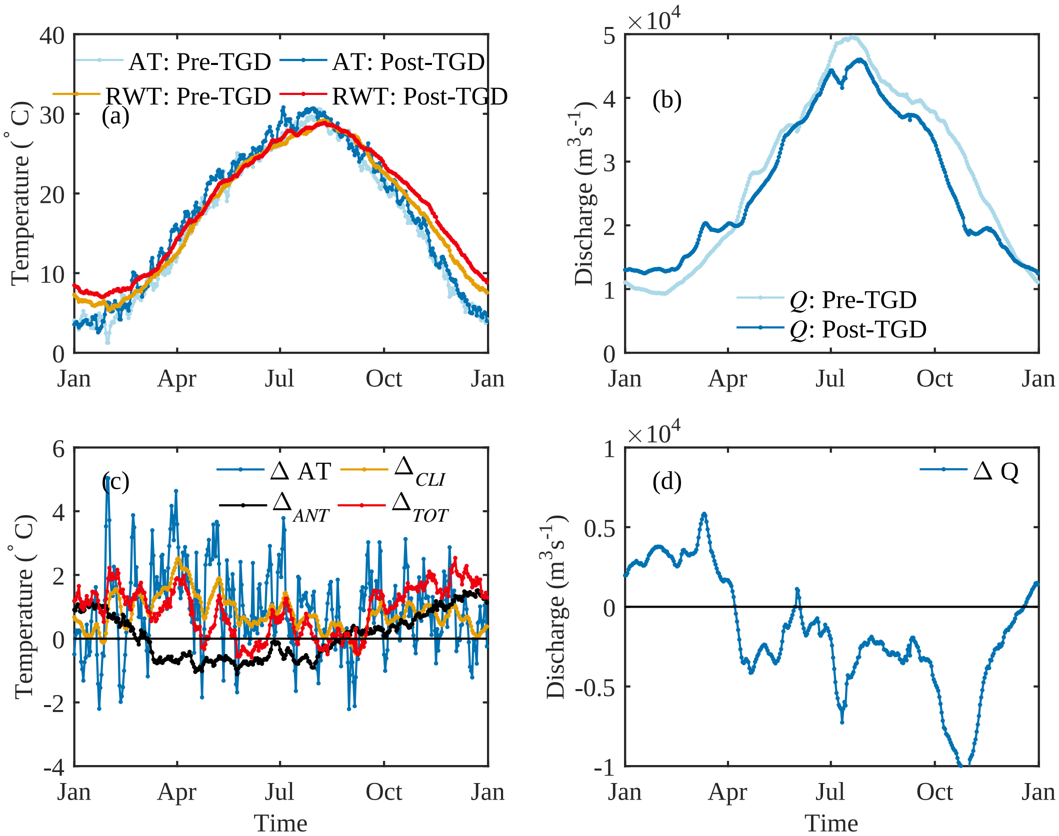

Figure S10. Seasonal dynamics (climatological year) of (a) AT and RWT, and (b) discharge Q, at Datong station during pre-TGD and post-TGD periods. Plots (c) and (d) show the differences between the two periods, highlighting the RWT changes caused by meteorological forcing and TGD.